

Journal of Research in Engineering, Volume 6, Number 2, 2009  
ISSN: 1591-8001  
**DYNAMIC BEHAVIORAL MODEL DEVELOPMENT FOR CONSTANT-FORCE  
COMPRESSION SPRING ELECTRICAL CONTACTS**

**Ikechukwu Celestine UGWUOKE, Matthew Sunday ABOLARIN, and  
Obiajulu Vincent OGWUAGWU**

Department of Mechanical Engineering,  
Federal University of Technology, Minna, Niger State, Nigeria.

E-mail(s): [ugwuokeikechukwu@yahoo.com](mailto:ugwuokeikechukwu@yahoo.com), [abolarinmatthew@yahoo.com](mailto:abolarinmatthew@yahoo.com)  
[ovogwuagwu@yahoo.com](mailto:ovogwuagwu@yahoo.com)

### **ABSTRACT**

*This research work explores the usefulness of the pseudo-rigid-body model (PRBM) in the dynamic behaviour analysis of constant-force compression spring electrical contacts (CFCSECs). It also expresses the desire to understand how CFCSECs behave dynamically. Such knowledge is important in the implementation of CFCSECs in viable commercial applications. The relative simplicity of employing the PRBM to streamline the dynamic analysis of CFCSECs, compared with existing dynamical methods, combined with the fact that the dynamic model can be represented mathematically, is a large step forward. Results obtained for these CFCSECs revealed a very important phenomenon of the peak-to-peak force plot, that over certain range of frequencies, these mechanisms exhibit better constant-force behaviour than they do statically.*

**Key word:** *Usefulness of the PRBM, viable commercial applications, streamline the dynamic analysis, dynamical methods*

### **INTRODUCTION**

Designing compliant mechanisms (CMs) for specific applications can be a complex problem with many considerations. The basic trade-off is between the flexibility to achieve deformed motion and the rigidity to sustain external load (Li and Kota, 2002). The impact of dynamic behaviour is of great importance in improving the design of CMs, especially for complex mechanisms and for micro-electro mechanical systems (MEMS) (Wang and Yu, 2007). The dynamics of mechanisms that include flexible links has received a lot of consideration in the last years, directly reflecting the increase in both the number and scope of applications for which the dynamic response must be accurately modeled in order to ensure that the mechanisms operate properly in the dynamic range (Lobontiu, 2003). Although existing methods such as the finite element method (FEM), elliptic integrals method, and chain algorithm method are widely available, there remain challenges in the computational model of CMs (Lan, 2005). This research work expresses the desire to understand how constant-force compression spring electrical contacts (CFCSECs) behave dynamically. Such knowledge is important in the implementation of CFCSECs in viable commercial applications. This understanding is attempted by using the pseudo-rigid-body (PRB) modeling technique. The PRBM is a design tool that approximates the force-deflection relationships of CMs by assigning a rigid-body, lumped compliance counterpart to every flexible segment comprising the mechanism (Howell, 2001). What makes it so useful is its ability to transform a CM requiring in-depth nonlinear analysis into an "equivalent" rigid-body mechanism, for which well-known rigid-body kinematics techniques are already in place. Though the PRBM has been shown to be valid for the static analysis of CMs, very little research has been performed to explore its usefulness in dynamic analysis (Boyle, 2001). If the model can be shown to approximate well the dynamic response of CFCSECs, then its usefulness is extended even further.

### **DEVELOPMENTAL ANALYSIS**

Figures 1 show the different configurations of CFCSEC. As shown in the figure, Class 3A mechanisms are basically CFCSECs that have three flexible segments located at the first, second, and third pivot points. Figure 2 shows the CFCSEC Configuration *Class 3A – III* and its PRBM.

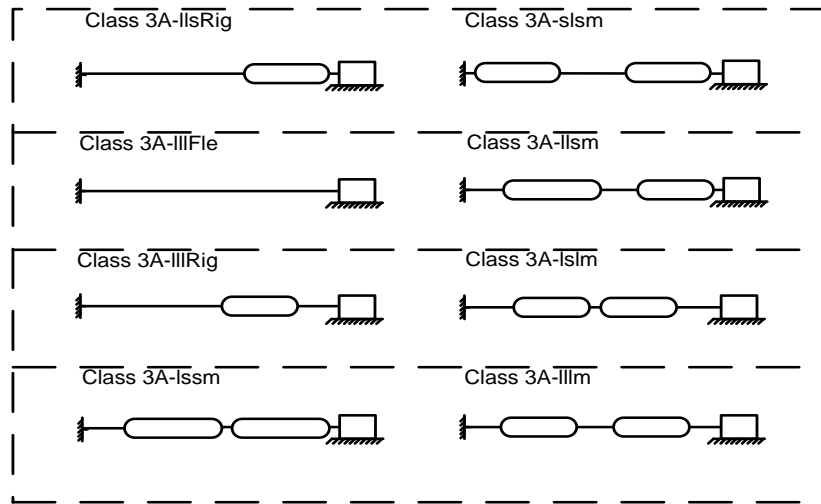


Figure 1: Developed Configurations of CFCSECs

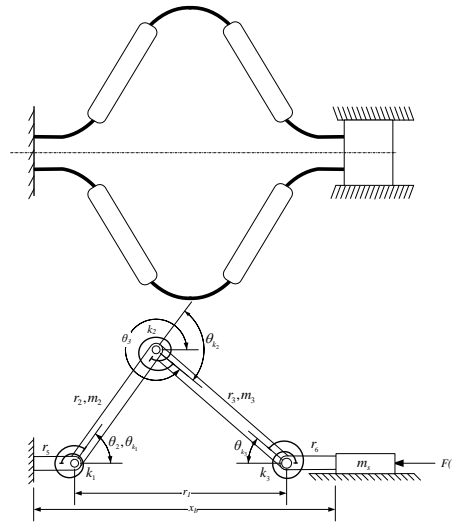


Figure 2: CFCSEC Configuration *Class 3A – IIIm* and the Generalized PRBM

**THE GENERALIZED PSEUDO-RIGID-BODY MODEL (PRBM)**

The generalized PRBM for all CFCSEC configurations is shown in Figure 2; only half of the symmetric mechanism is shown. The lengths of the rigid segments, placement of the pin joints, and the spring constants of the torsional springs may all be calculated using various model parameters. The generalized expression for the torsional spring constant  $k$  for the flexible segments of the different configurations of CFCSEC is given by

$$k = n\gamma K_{\theta} \frac{EI}{L} \tag{1}$$

where  $\gamma$  is the PRBM characteristic radius factor,  $K_{\theta}$  is the torsional spring stiffness coefficient,  $E$  is the modulus of elasticity of the flexible segment,  $I$  is the moment of inertia of the cross section of the flexible segment,  $L$  is the length of the flexible segment. The average values for  $\gamma$  and  $K_{\theta}$  over a wide range of loading conditions have been tabulated (Howell and Midha, 1995), but may be approximated for any material properties as 0.85 and 2.65 respectively for long flexible segments and for short flexural pivots, the values of  $\gamma$  and  $K_{\theta}$  are 1. For long fixed-fixed flexible segment  $n = 2$  and for long fixed-pinned flexible segment and short flexural pivot,  $n = 1$ . The variable  $x_b$  is simply a measurement of the point where the mechanism attaches to the slider located with respect to where the mechanism connects to ground. The following expressions, along with the definition

given in Figure 3, may be used to determine the lengths of the flexible and rigid segments for the different CFCSEC configurations.

$$r_{Tot} = r_2 + r_3 = \text{Total PRBM length} \quad (2)$$

$$r_2 = \frac{r_{Tot}}{(R+1)} \quad (3)$$

$$r_3 = \frac{r_{Tot}}{\left(\frac{1}{R} + 1\right)} \quad (4)$$

$$R = \frac{r_3}{r_2} = \text{Geometric parameter ratio} \quad (5)$$

$$\lambda = \frac{L_{Tot}}{r_{Tot}} = \text{Length parameter ratio} \quad (6)$$

$L_{Tot}$  = Total length of actual CCFCM

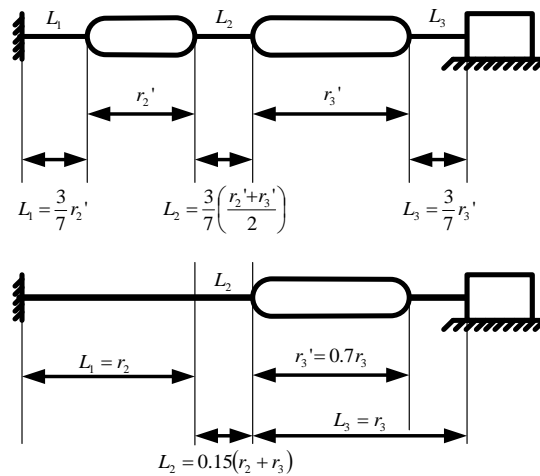


Figure 3: Definition of flexible and rigid segment lengths

### DYNAMIC BEHAVIORAL MODEL FORMULATION USING LAGRANGE'S METHOD

Lagrange's method is one of the most useful techniques in generating equations of motion of CMs, especially when internal forces and reactions are not of interest. For CFCSECs, the particular interest in a dynamic analysis is its output force. Taking  $\theta_2$  as the generalized position coordinate and neglecting the effect of damping on the CFCSEC PRBM, Lagrange's equation is expressed as (Sandor and Erdman, 1988)

$$\frac{d}{dt} \left( \frac{\partial(T-V)}{\partial \dot{\theta}_2} \right) - \frac{\partial(T-V)}{\partial \theta_2} = Q_{\theta_2} \quad (7)$$

where,

$Q_{\theta_2}$  = Generalized force

Using the PRBM, the potential energy equation can easily be obtained. For a segment modeled using a torsional spring and a pin joint, the total potential energy in the mechanism (assuming negligible potential energy due to gravity) is the sum of the individual potential energy stored in each compliant segment.

$$V = \sum_{i=2}^n V_i = \frac{1}{2} \sum_{i=2}^n (k_i \theta_{ki}^2) \quad (8)$$

where  $i = 2, 3, \dots, n$  enumerates all torsional springs

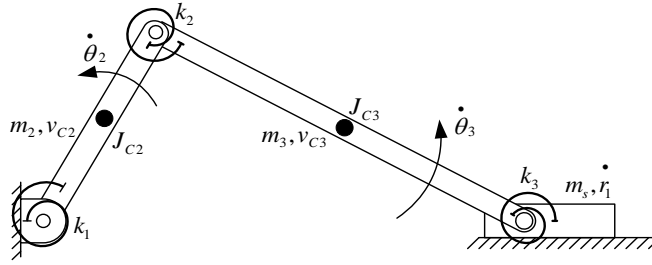


**Figure 4:** Translational and rotational motion of the mechanism link

As shown in Figure 4, the centre of mass of each link translates along a predefined path with linear velocity as the mechanism moves, and each link is also rotating about its centre of mass with angular velocity. The total kinetic energy for any given link is therefore, the sum of the translational and rotational kinetic energies.

$$T = \sum_{i=2}^n T_i = \frac{1}{2} \sum_{i=2}^n \left( m_i V_{Ci}^2 + J_{Ci} \dot{\theta}_i^2 \right) \quad (9)$$

Where  $i = 2, 3, \dots, n$  enumerates all moving links.

For CFCSECs, the generalized forcing function  $Q_{\theta_2}$  consists of a moment  $\tau_F$  due directly to the force  $F$  acting on the slider and the term  $\tau_{AF}$  is introduced to compensate for the moment due to axial force effects in the mechanism's links/segments. In mathematical terms, the generalized forcing function  $Q_{\theta_2}$  may be expressed as follows

$$Q_{\theta_2} = \tau_F + \tau_{AF} \quad (10)$$

The value of the torque  $\tau_{AF}$  is approximated using the expression giving below

$$\tau_{AF} = F \delta e = F_{static} r_2 \alpha \left( 1 + \frac{r_2}{\sqrt{r_3^2 - r_2^2 \alpha^2}} \right) \quad \alpha \text{ is the angle of axial force effect} \quad (11)$$

The value of  $\alpha$  is chosen using experimental data from static tests. Expanding out equation (7) and simplifying, the generalized dynamic equation of motion for CFCSECs becomes

$$\begin{aligned}
 & \left[ m_2 \left( \left( \frac{1}{3} \right) r_2^2 \right) + m_3 \left( \frac{r_2^3 \sin^2 \theta_2 \cos \theta_2}{\sqrt{r_3^2 - r_2^2 \sin^2 \theta_2}} + \left( \frac{1}{3} \right) \frac{r_2^2 r_3^2 \cos^2 \theta_2}{r_3^2 - r_2^2 \sin^2 \theta_2} + r_2^2 \sin^2 \theta_2 \right) \right. \\
 & + m_s \left( \frac{r_2^4 \sin^2 \theta_2 \cos^2 \theta_2}{r_3^2 - r_2^2 \sin^2 \theta_2} + 2 \frac{r_2^3 \sin^2 \theta_2 \cos \theta_2}{\sqrt{r_3^2 - r_2^2 \sin^2 \theta_2}} + r_2^2 \sin^2 \theta_2 \right) \left. \right] \ddot{\theta}_2 \\
 & + \left[ m_3 \left( \left( \frac{1}{2} \right) \frac{r_2^5 \sin^3 \theta_2 \cos^2 \theta_2}{(r_3^2 - r_2^2 \sin^2 \theta_2)^{3/2}} + \left( \frac{1}{3} \right) \frac{r_2^4 r_3^2 \sin \theta_2 \cos^3 \theta_2}{(r_3^2 - r_2^2 \sin^2 \theta_2)^2} - \left( \frac{1}{2} \right) \frac{r_2^3 \sin^3 \theta_2}{\sqrt{r_3^2 - r_2^2 \sin^2 \theta_2}} \right. \right. \\
 & + \left. \frac{r_2^3 \sin \theta_2 \cos^2 \theta_2}{\sqrt{r_3^2 - r_2^2 \sin^2 \theta_2}} - \left( \frac{1}{3} \right) \frac{r_2^2 r_3^2 \sin \theta_2 \cos \theta_2}{r_3^2 - r_2^2 \sin^2 \theta_2} + r_2^2 \sin \theta_2 \cos \theta_2 \right) \\
 & + m_s \left( \frac{r_2^6 \sin^3 \theta_2 \cos^3 \theta_2}{(r_3^2 - r_2^2 \sin^2 \theta_2)^2} + \frac{r_2^5 \sin^3 \theta_2 \cos^2 \theta_2}{(r_3^2 - r_2^2 \sin^2 \theta_2)^{3/2}} - \frac{r_2^4 \sin^3 \theta_2 \cos \theta_2}{r_3^2 - r_2^2 \sin^2 \theta_2} \right. \\
 & + \left. \frac{r_2^4 \sin \theta_2 \cos^3 \theta_2}{r_3^2 - r_2^2 \sin^2 \theta_2} + 2 \frac{r_2^3 \sin \theta_2 \cos^2 \theta_2}{\sqrt{r_3^2 - r_2^2 \sin^2 \theta_2}} - \frac{r_2^3 \sin^3 \theta_2}{\sqrt{r_3^2 - r_2^2 \sin^2 \theta_2}} + r_2^2 \sin \theta_2 \cos \theta_2 \right) \left. \right] \dot{\theta}_2^2 \\
 & + k_1 \theta_2 + k_2 \left( \theta_2 + \sin^{-1} \left( \frac{r_2}{r_3} \sin \theta_2 \right) \right) \left( 1 + \frac{r_2 \cos \theta_2}{\sqrt{r_3^2 - r_2^2 \sin^2 \theta_2}} \right) \\
 & + k_3 \left( \sin^{-1} \left( \frac{r_2}{r_3} \sin \theta_2 \right) \right) \left( \frac{r_2 \cos \theta_2}{\sqrt{r_3^2 - r_2^2 \sin^2 \theta_2}} \right) - F_{static} r_2 \alpha \left( 1 + \frac{r_2}{\sqrt{r_3^2 - r_2^2 \alpha^2}} \right) = \tau_F
 \end{aligned} \tag{12}$$

Torque  $\tau_F$  is transformed to mechanism's output force  $F$  using the power relationship given by

$$F \dot{r}_1 = F \dot{\theta}_2 \left( -r_2 \sin \theta_2 - \frac{r_2^2 \sin \theta_2 \cos \theta_2}{\sqrt{r_3^2 - r_2^2 \sin^2 \theta_2}} \right) = \tau_F \dot{\theta}_2 \tag{13}$$

### EQUATIONS FORMULATION USING THE PRINCIPLE OF VIRTUAL WORK

The concept of virtual work is another useful device for solving both static and quasi-static force analysis problems. Virtual work, however, refers to imagined work, the displacement does not actually occur, it is introduced as an imagined quantity (Sandor and Erdman, 1988). A mechanism with rigid components is in a state of static equilibrium if the sum of the virtual work done by all real forces and moments is zero for every virtual displacement consistent with the kinematics constraints. If elastic components are a part of the mechanical system, the total virtual work done by these elastic components is equal to the total virtual work of all real forces and moments (acting on the non elastic components) for virtual displacement consistent with the constraint (Sandor and Erdman, 1988). Thus for such a system

$$\sum_i (F_i \bullet \delta s_i) + \sum_j (M_j \bullet \delta \phi_j) = \sum_k \left( \frac{\partial V_k}{\partial q_k} \right) \delta q_k \tag{14}$$

Application of the principle of virtual work to the generalized CFCSEC PRBM and taking the variable  $\theta_2$  as the generalized position coordinate, gives the following expression

$$F_{vw} = \frac{1}{r_2 r_3 \sin(\theta_2 - \theta_3)} \left( k_1 r_3 \theta_2 \cos \theta_3 + k_2 \theta_{k_2} (r_2 \cos \theta_2 + r_3 \cos \theta_3) + k_3 r_2 \theta_{k_3} \cos \theta_2 \right) \tag{15}$$

### RESULTS AND DISCUSSIONS

The relevant mechanism parameters and variable values for the different CFCSEC configuration are given in Table 1. The variables b, h, and I are the width, the thickness, and the area moment of inertia of the flexible segment's cross section; E is the modulus of elasticity of the flexible segments. As shown in Figure 5, a comparison of the force predicted by the static portion of the dynamic model with velocities and accelerations set to zero (with

$\tau_{AF} = 0$ ), for a 10 and 15% displacement, with that predicted by existing compliant mechanism theory, essentially an application of the principle of virtual work on the PRBM of CFCSEC configuration *Class 3A – III<sub>m</sub>*, shows that both plots match perfectly, which is a confirmation that the static portion of the dynamic model is correct. Figure 6, 7 and 8 shows the force displacement diagram showing the force predicted by the static portion of the dynamic model for the different CFCSEC configurations, the percent constant-force prediction plot and the model force prediction plot as a function of time for the different CFCSEC configurations respectively for a 10 and 15% displacement. In the evaluation of the generalized dynamic model for its constant-force capabilities, three useful plots were analyzed, which includes, the mean force plots, the median force plots, and the peak-to-peak force plots shown in Figure 9, 10, and 11 respectively as a function of frequency. Notice that each curve in the peak-to-peak force plot first curves down, before it starts to increase. This dip in the peak-to-peak force shows the range of frequencies over which CFCSECs exhibits better constant-force behaviour than they do statically. In fact, the same observation was made by Boyle (2001) while studying the dynamics of compliant constant-force mechanisms. The results for a single frequency with very low peak-to-peak force have been tabulated as shown in Table 2 for a 10, 15, and 20% displacement respectively. The percent constant-force (PCF) may be obtained using the expression

$$PCF = 100 \times \left( \frac{\min(F_{\text{modeled}})}{\max(F_{\text{modeled}})} \right) \quad (16)$$

Multiplying by a hundred gives the PCF as a percentage with 100% being perfectly constant. The PCF is very important because it measures the amount of variation between the minimum and maximum output force of the CFCSEC. Due to the nature of CFCSECs, the maximum force is usually located at the maximum deflection and the minimum force can generally be found at the smallest deflection.

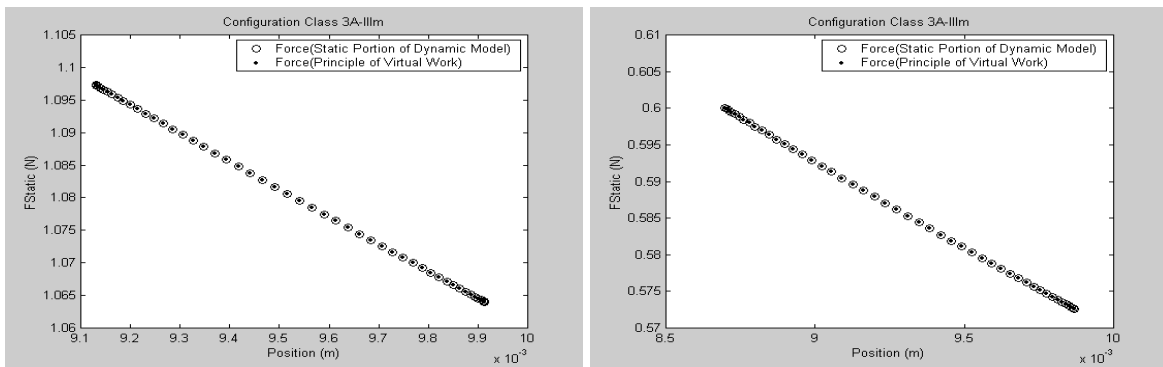


**Figure 5:** Comparison of the force predicted by the static portion of the dynamic model with that predicted by the principle of virtual work for CFCSEC configuration *Class 3A – III<sub>m</sub>*

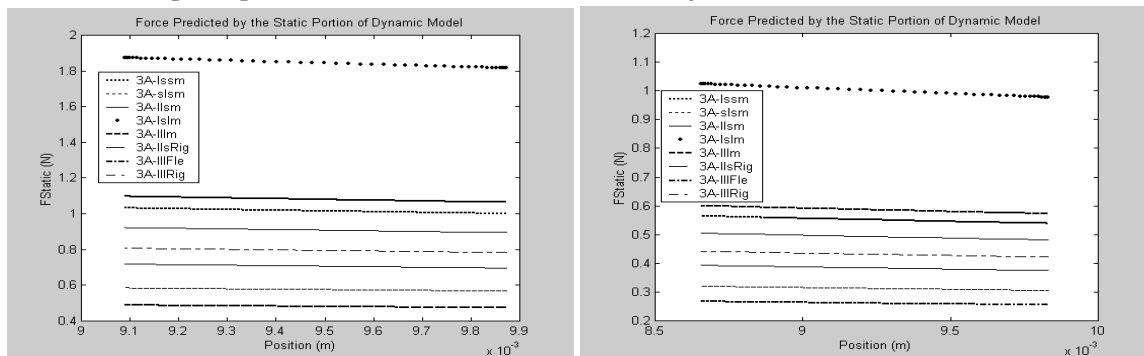


**Figure 6:** Force displacement diagram showing the force predicted by the static portion of the dynamic model for a 10 and 15% displacement of the different CFCSEC configurations

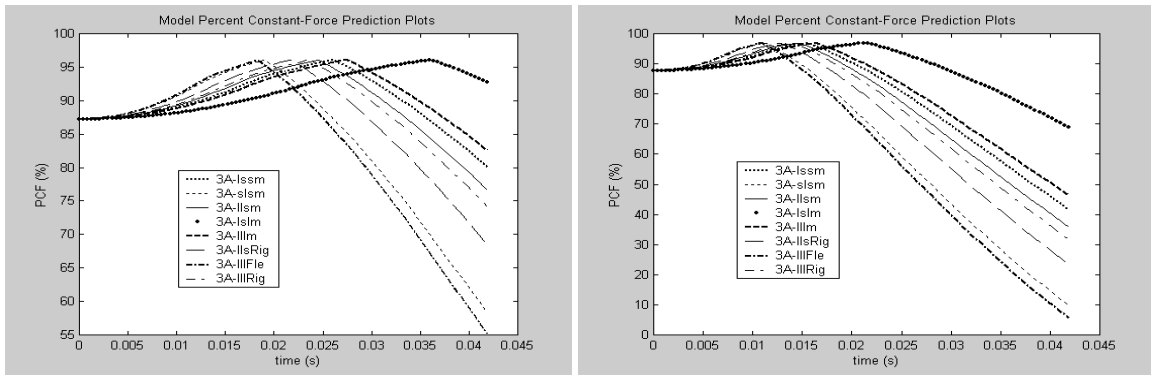


**Figure 7:** Percent constant-force prediction plot as a function of time for a 10 and 15% displacement of the different CFCSEC configurations

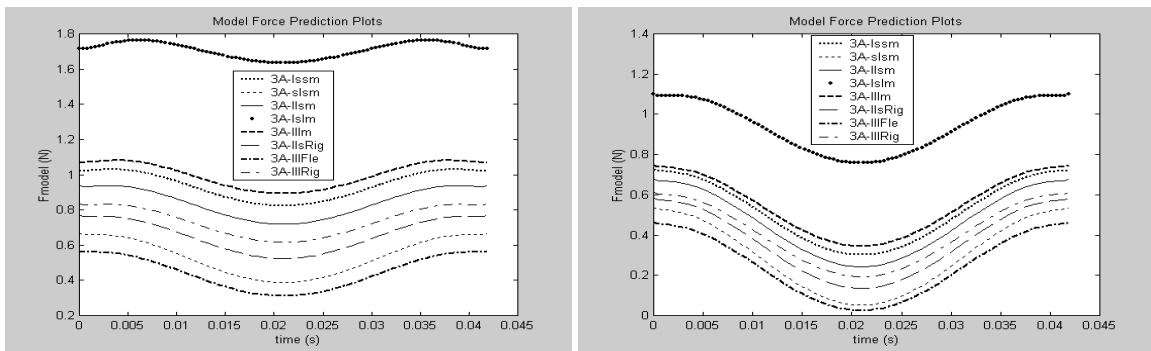


**Figure 8:** Model force prediction plot as a function of time for a 10 and 15% displacement of the different CFCSEC configurations

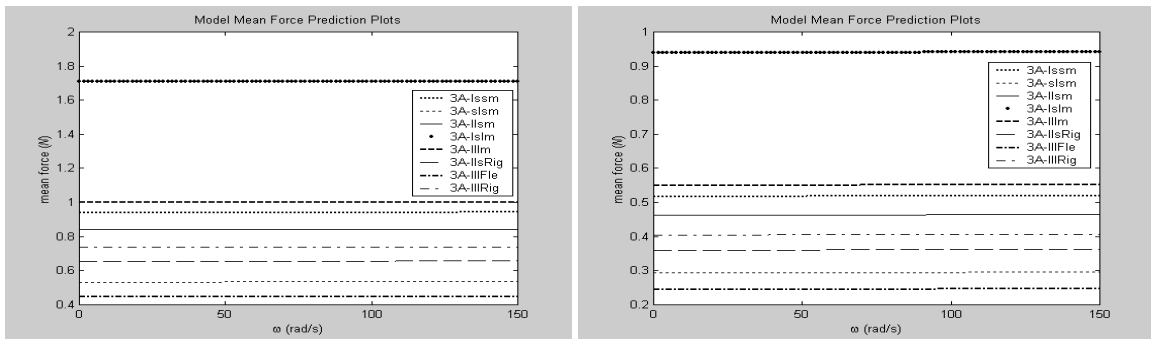


**Figure 9:** Mean force plot as a function of frequency for a 10 and 15% displacement of the different CFCSEC configurations

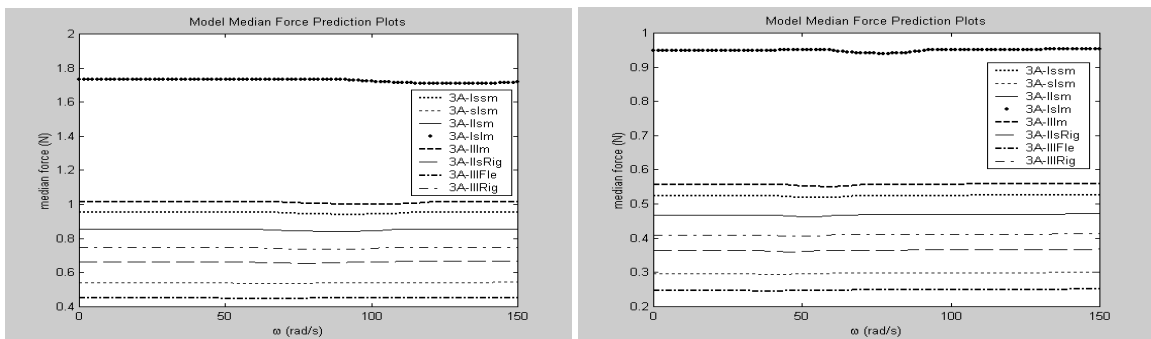


**Figure 10:** Median force plot as a function of frequency for a 10 and 15% displacement of the different CFCSEC configurations

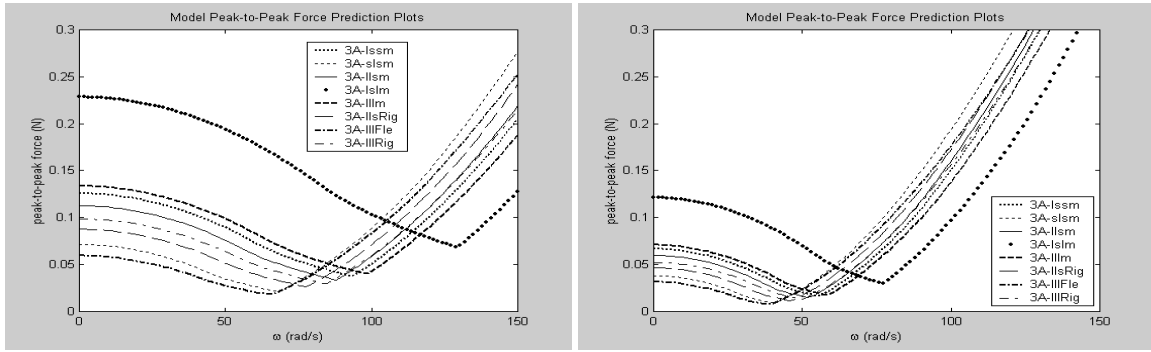


**Figure 11:** Peak-to-peak force plot as a function of frequency for a 10 and 15% displacement of the different CFCSEC configurations

**TABLE 1:** Parameters and variable values for the different configurations of CFCSECs

| Parameter   | Class 3A – lssm | Class 3A – slsm  | Class 3A – llsm  | Class 3A – lslm  |
|-------------|-----------------|------------------|------------------|------------------|
| $r_2$       | 4.5165 mm       | 4.8077 mm        | 4.5699 mm        | 4.2757 mm        |
| $r_3$       | 4.5165 mm       | 4.8077 mm        | 4.5699 mm        | 4.2757 mm        |
| $r_5$       | 0.7631 mm       | -                | 0.6775 mm        | 0.7247 mm        |
| $r_6$       | -               | -                | -                | 0.7247 mm        |
| $m_2$       | 0.0168 g        | 0.0166 g         | 0.0153 g         | 0.0158 g         |
| $m_3$       | 0.0164 g        | 0.0166 g         | 0.0157 g         | 0.0158 g         |
| $m_s$       | 8.7535 g        | 8.7535 g         | 8.7535 g         | 8.7535 g         |
| $b$         | 5 mm            | 5 mm             | 5 mm             | 5 mm             |
| $h_{Solid}$ | 0.1 mm          | 0.1 mm           | 0.1 mm           | 0.1 mm           |
| $h_1$       | 0.0457 mm       | 0.0085 mm        | 0.0312 mm        | 0.0434 mm        |
| $h_2$       | 0.0043 mm       | 0.0244 mm        | 0.0219 mm        | 0.0038 mm        |
| $h_3$       | 0.0092 mm       | 0.0085 mm        | 0.0082 mm        | 0.0434 mm        |
| $E$         | 110 GPa         | 110 GPa          | 110 GPa          | 110 GPa          |
| $S_Y$       | 552 Mpa         | 552 Mpa          | 552 Mpa          | 552 Mpa          |
| $l_1$       | 1.5263 mm       | 0.3803 mm        | 1.3551 mm        | 1.4494 mm        |
| $l_2$       | 0.3840 mm       | 1.6297 mm        | 1.4611 mm        | 0.3382 mm        |
| $l_3$       | 0.4119 mm       | 0.3803 mm        | 0.3657 mm        | 1.4494 mm        |
| $k_1$       | 4.2599 mNm      | 0.1461 mNm       | 1.9905 mNm       | 3.8414 mNm       |
| $k_2$       | 0.0186 mNm      | 0.6071 mNm       | 0.4880 mNm       | 0.0144 mNm       |
| $k_3$       | 0.1714 mNm      | 0.1461 mNm       | 0.1351 mNm       | 3.8414 mNm       |
| Parameter   | Class 3A – lllm | Class 3A – llRig | Class 3A – llFle | Class 3A – llRig |
| $r_2$       | 4.3478 mm       | 4.5528 mm        | 4.3478           | 4.3478 mm        |
| $r_3$       | 4.3478 mm       | 4.5528 mm        | 4.3478 mm        | 4.3478 mm        |
| $r_5$       | 0.6522 mm       | 0.6711 mm        | 0.6319 mm        | 0.6319 mm        |
| $r_6$       | 0.6522 mm       | -                | 0.6319 mm        | 0.6319 mm        |
| $Rig$       | -               | 3.6215 mm        | -                | 2.9487 mm        |
| $m_2$       | 0.0143 g        | 0.0083 g         | 0.0060 g         | 0.0060 g         |
| $m_3$       | 0.0143 g        | 0.0157 g         | 0.0060 g         | 0.0145 g         |
| $m_s$       | 8.7535 g        | 8.7535 g         | 8.7535 g         | 8.7535 g         |
| $b$         | 5 mm            | 5 mm             | 5 mm             | 5 mm             |
| $h_{Solid}$ | 0.1 mm          | 0.1 mm           | 0.1 mm           | 0.1 mm           |
| $h_1$       | 0.0301 mm       | 0.0232 mm        | 0.0177 mm        | 0.0177 mm        |
| $h_2$       | 0.0150 mm       | 0.0232 mm        | 0.0177 mm        | 0.0177 mm        |
| $h_3$       | 0.0301 mm       | 0.0081 mm        | 0.0177 mm        | 0.0291 mm        |
| $l_1$       | 1.3043 mm       | 4.4740 mm        | 4.2124 mm        | 4.2124 mm        |

|       |            |            |            |            |
|-------|------------|------------|------------|------------|
| $l_2$ | 1.3043 mm  | 5.1736 mm  | 5.1151 mm  | 5.1151 mm  |
| $l_3$ | 1.3043 mm  | 0.3622 mm  | 4.2124 mm  | 4.2124 mm  |
| $k_1$ | 1.8443 mNm | 0.8270 mNm | 0.3875 mNm | 0.3875 mNm |
| $k_2$ | 0.2305 mNm | 0.5506 mNm | 0.3191 mNm | 0.3191 mNm |
| $k_3$ | 1.8443 mNm | 0.1325 mNm | 0.3875 mNm | 1.7312 mNm |

**TABLE 2:** Summary of simulation results for a 10% displacement of the different configurations of CFCSEC

| Configuration            | R   | PCF Static (%) | PCF Dynamic (%) | Mean Force Static (N) | Mean Force Dynamic (N) | STDev Static | STDev Dynamic |
|--------------------------|-----|----------------|-----------------|-----------------------|------------------------|--------------|---------------|
| <b>10% Displacement</b>  |     |                |                 |                       |                        |              |               |
| <i>Class 3A – lssm</i>   | 1.0 | 96.9681        | 96.0687         | 1.0163                | 0.9413                 | 0.0112       | 0.0141        |
| <i>Class 3A – slsm</i>   | 1.0 | 96.9681        | 96.0611         | 0.5765                | 0.5339                 | 0.0063       | 0.0082        |
| <i>Class 3A – llsm</i>   | 1.0 | 96.9681        | 96.0531         | 0.9090                | 0.8418                 | 0.0100       | 0.0124        |
| <i>Class 3A – lslm</i>   | 1.0 | 96.9681        | 96.0523         | 1.8443                | 1.7081                 | 0.0203       | 0.0246        |
| <i>Class 3A – llm</i>    | 1.0 | 96.9681        | 96.0689         | 1.0803                | 1.0005                 | 0.0119       | 0.0142        |
| <i>Class 3A – llsRig</i> | 1.0 | 96.9681        | 96.0631         | 0.7075                | 0.6553                 | 0.0078       | 0.0103        |
| <i>Class 3A – llFle</i>  | 1.0 | 96.9681        | 96.0500         | 0.4806                | 0.4451                 | 0.0053       | 0.0068        |
| <i>Class 3A – llRig</i>  | 1.0 | 96.9681        | 96.0699         | 0.7955                | 0.7367                 | 0.0087       | 0.0116        |
| <b>15% Displacement</b>  |     |                |                 |                       |                        |              |               |
| <i>Class 3A – lssm</i>   | 1.0 | 95.4269        | 96.8727         | 0.5513                | 0.5180                 | 0.0092       | 0.0059        |
| <i>Class 3A – slsm</i>   | 1.0 | 95.4269        | 96.7862         | 0.3127                | 0.2938                 | 0.0052       | 0.0031        |
| <i>Class 3A – llsm</i>   | 1.0 | 95.4269        | 96.8508         | 0.4930                | 0.4632                 | 0.0082       | 0.0051        |
| <i>Class 3A – lslm</i>   | 1.0 | 95.4269        | 96.8890         | 1.0004                | 0.9399                 | 0.0167       | 0.0110        |
| <i>Class 3A – llm</i>    | 1.0 | 95.4269        | 96.8820         | 0.5860                | 0.5506                 | 0.0098       | 0.0064        |
| <i>Class 3A – llsRig</i> | 1.0 | 95.4269        | 96.8491         | 0.3838                | 0.3606                 | 0.0064       | 0.0043        |
| <i>Class 3A – llFle</i>  | 1.0 | 95.4269        | 96.8486         | 0.2607                | 0.2449                 | 0.0044       | 0.0030        |
| <i>Class 3A – llRig</i>  | 1.0 | 95.4269        | 96.8470         | 0.4315                | 0.4054                 | 0.0072       | 0.0045        |
| <b>20% Displacement</b>  |     |                |                 |                       |                        |              |               |
| <i>Class 3A – lssm</i>   | 1.0 | 93.8681        | 97.3670         | 0.3568                | 0.3381                 | 0.0081       | 0.0038        |
| <i>Class 3A – slsm</i>   | 1.0 | 93.8681        | 97.3834         | 0.2024                | 0.1918                 | 0.0046       | 0.0018        |
| <i>Class 3A – llsm</i>   | 1.0 | 93.8681        | 97.3625         | 0.3191                | 0.3024                 | 0.0072       | 0.0036        |
| <i>Class 3A – lslm</i>   | 1.0 | 93.8681        | 97.3852         | 0.6474                | 0.6135                 | 0.0146       | 0.0058        |
| <i>Class 3A – llm</i>    | 1.0 | 93.8681        | 97.4066         | 0.3793                | 0.3594                 | 0.0086       | 0.0040        |
| <i>Class 3A – llsRig</i> | 1.0 | 93.8681        | 97.4002         | 0.2484                | 0.2354                 | 0.0056       | 0.0026        |
| <i>Class 3A – llFle</i>  | 1.0 | 93.8681        | 97.3555         | 0.1687                | 0.1599                 | 0.0038       | 0.0015        |
| <i>Class 3A – llRig</i>  | 1.0 | 93.8681        | 97.3549         | 0.2793                | 0.2646                 | 0.0063       | 0.0030        |

**CONCLUSION**

The field of compliant mechanisms (CMs) is relatively new, and many design research issues are still unanswered. As the research matures in this area, we can expect to identify more and more applications of CMs in the near future. Although there are existing methods for the analysis of CMs, such as the finite element method, the elliptic integral method, and the chain algorithm method, there are still challenges in the computational models of CMs.

Many of these existing methods in most cases do not consider dynamic effect in the design stage. Therefore the resulting designs are valid for static or low frequency applications only. This research work expresses the desire to understand how constant-force compression spring electrical contacts (CFCSECs) behave dynamically. Such knowledge is important in the implementation of CFCSECs in viable commercial applications. This understanding was attempted using the pseudo-rigid-body modeling technique. The relative simplicity of employing the PRBM to streamline the dynamic analysis, compared with existing dynamical methods, combined with the fact that the dynamic model can be represented mathematically, is a large step forward. Results obtained for these CFCSECs revealed a very important phenomenon of the peak-to-peak force plot, that over certain range of frequencies, these mechanisms exhibit better constant-force behaviour than they do statically.

### REFERENCES

- [1] Boyle CL (2001) A Closed-Form Dynamic Model of the Compliant Constant-Force Mechanism using the Pseudo-Rigid-Body Model. M.S. Thesis, Brigham Young University, Provo, Utah.
- [2] Howell LL (2001) Compliant Mechanisms. John Wiley & Sons, New York.
- [3] Howell LL and Midha A (1995) Parametric Deflection Approximations for End-Loaded, Large-Deflection Beams in Compliant Mechanisms. ASME Journal of Mechanical Design, Vol. 117, No. 1, pp. 156-165.
- [4] Li Z and Kota S (2002) Dynamic Analysis of Compliant Mechanisms. Proceedings of the ASME Design Engineering Technical Conference, Vol. 5, pp. 43-50.
- [5] Lan C (2005) Computational Models for Design and Analysis of Compliant Mechanisms. Ph.D Dissertation, Georgia Institute of Technology.
- [6] Lobontiu N (2003) Compliant Mechanisms: Design of Flexure Hinges. CRC Press LLC, Boca Raton, USA.
- [7] Sandor GN and Erdman AG (1988) Advanced Mechanism Design: Analysis and Synthesis. Volume 2, Prentice-Hall, New Delhi, pp. 435-530.
- [8] Wang W and Yu Y (2007) Analysis of Frequency Characteristics of Compliant Mechanisms. Front. Mech. Eng. China 2007, 2(3), pp. 267-271.